COMMUNICATION

Direct Observation of Quantum-Confined Graphene-Like States and Novel Hybrid States in Graphene Oxide by Transient Spectroscopy

Lei Wang, Hai-Yu Wang,* Yan Wang, Shou-Jun Zhu, Yong-Lai Zhang, Jun-Hu Zhang, Qi-Dai Chen, Wei Han, Huai-Liang Xu, Bai Yang, and Hong-Bo Sun*

Graphene oxide (GO) has attracted broad interest as a feasible, one-atom-thick, two-dimensional prototype material in organic optical–electronic devices and biosensors.[1–7] It not only contains local sp² domains, which are analogues of graphitic crystalline graphene with high carrier transport mobility,[8–10] but also possesses sp³-hybridized carbon atoms that are bound to plentiful oxygen-containing functional groups on the basal plane and sheet edge, which can interact with strong light absorbers or emitters (that is, dyes, polymers, and nanoparticles).[11–18] Originally, it was thought that through removal of oxygen atoms on GO via chemical or thermal reduction, large-scale production of graphene sheets could be readily fabricated.[19,20] Unfortunately, remaining defects still exist widely in reduced GO (rGO).[21] These unwanted holes and functionalities are randomly distributed in GO/rGO,[22] making the discussion on electronic structure of graphene oxide elusive. Thus, one key question is especially hard to settle: electronically, how can we more reliably describe the interplay between the sp² domains and sp³ matrix in close vicinity?

These quantum-confined graphene-like states were at first viewed simply as finite fused aromatic rings, which have a size-dependent bandgap according to theoretical calculation.[23] Later on, on the basis of the experimental results from high-resolution transmission electron microscopy (TEM),[21,22] a large number of theoretical models about the role of functional groups in GO/rGO were proposed, in which these functional groups referring to sp³-hybridized carbon atoms strongly affected the optical–electronic properties.[24–30] In

L. Wang, Prof. H.-Y. Wang, Y.-L. Zhang,
Prof. Q. D. Chen, Prof. H. L. Xu, Prof. H. B. Sun
State Key Laboratory on Integrated Optoelectronics
College of Electronic Science and Engineering
Jilin University
2699 Qianjin Street, Changchun 130012, China
E-mail: haiyu_wang@jlu.edu.cn; hbsun@jlu.edu.cn
Y. Wang, Prof. W. Han, Prof. H.-B. Sun
College of Physics
Jilin University
2699 Qianjin Street, Changchun 130012, China
S.-J. Zhu, J.-H. Zhang, Prof. B. Yang
State Key Laboratory of Supramolecular Structure and Materials,
College of Chemistry
Jilin University
2699 Qianjin Street, Changchun 130023, China

other experiments, owing to the photochemical activity of sp³ domains, GO is treated as a precursor of a series of carbon nanomaterials: for example, carbon nanotubes, carbon nanoparticles, and graphene quantum dots (GQDs).[31–33] Among these new derivatives of GO are fluorescent GQDs, which are tiny pieces of graphene decorated with functional groups fabricated by hydrothermally or electrochemically cutting GO and its reduction product;[34] these GQDs simplify the discussion on their photophysical properties to a considerable degree by abandoning the redundant sp³ matrix, in return for which high photoluminescence (PL) emission appears. We have studied in detail the PL mechanism in green fluorescence GQDs, in which bright molecule-like states and dark intrinsic states are responsible for the fluorescence emission.[35] We suggest the intrinsic electronic state in GQDs could be inherited from its precursor GO. However, the electronic structure of GO has still been difficult to understand, until now. The main problem is that the unique spectral character of quantum-confined graphene-like states, as well as the feature of the so-called "sp³ matrix", has never been directly observed.

Here, an exciting step for solving these problems is presented via selective excitation of GO and rGO with photothermal treatment in femtosecond time-resolved broadband transient absorption experiments (see sample preparation and description of transient signals in the Supporting Information). Since it is found that the initial sizes (2–3 nm) of quantum-confined graphene-like states in GO do not increase with reduction, but instead of the creation of new sp² domains,[1] transient spectral signals of confined graphene-like states in the visible range can be directly observed that should be independent of the initial degree of reduction of GO and hence independent on the preparations of samples. If this universal feature is observed and demonstrated, it will give us a greater understanding of the electronic nature of GO. At the same time, it will also be remarkably different from previous reports in the field of ultrafast spectroscopy for GO, which would usually involve only featureless excited-state absorption signals[36–38] or just emission[39]. According to our transient spectral evolution of GO/rGO, the experimental results about confined graphene-like states are highly consistent with previously expected universal features. Surprisingly, the spectral characterization of amorphous carbon-like matrix with high sp³/sp² carbon ratio in close vicinity of graphene-like states is further identified in GO at nearly 2.95 eV (420 nm), in comparison with photothermally reduced GO, in which this novel state is red-shifted to 2.85 eV
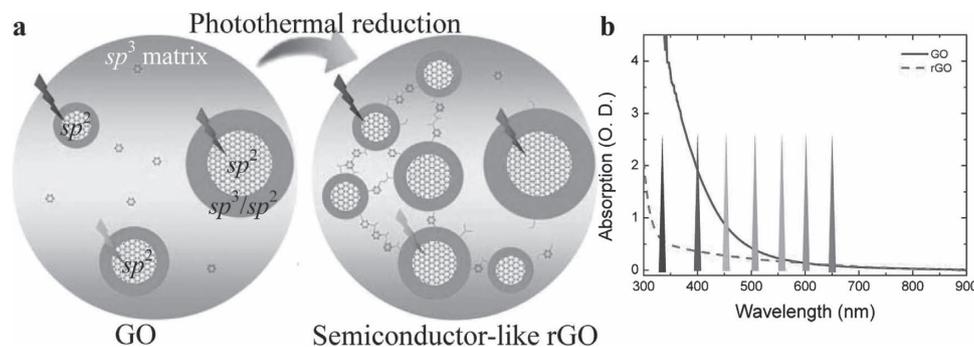
Figure 1. Brief guideline of selective excitation in GO/rGO. a) Fundamental physical picture for selective excitation in GO/rGO. The sp^3 matrix decorated with oxygen-containing functional groups is indicated in purple, graphitic areas with different size in green, which can be excited by corresponding pump lights, and the hybrid region with high sp^3/sp^2 ratio in orange. b) Steady-state absorption spectra of GO and rGO. The colored arrows indicate the different pump wavelengths in transient absorption experiments.

(435 nm). This hybrid state is commonly found to exist in various carbon nanomaterials including electrochemically fabricated carbon dots and solvothermally synthesized graphene quantum dots. In addition, the transient signals in respect of oxygen-containing functional groups are also discussed.

Figure 1a provides a brief guideline description of this project. By changing the pump wavelength in GO/rGO, the possibly existent quantum-confined graphene-like states in the visible range and oxygen-containing functional groups in sp^3 matrix in the ultraviolet range should be selectively excited. Comparing these transient spectra before and after reduction could answer these initial questions, as mentioned above. This is fundamental and normal but has never been done before. As the steady-state absorption spectroscopy shows (Figure 1b), the absorption of GO gradually decreases from ultraviolet to visible, until there are no clear absorption peaks at all. Femtosecond transient absorption spectroscopy is a powerful tool for exploring the hidden information on electronic structure of materials. In previous work, either the excitation in visible range was ignored,[36] or the probe window was too narrow to observe the full information.[37,38]

On the basis of our wide probe range from entirely visible to near-infrared light,[40–42] the femtosecond selective excitation experiments give us amazing results, as shown in **Figure 2**a–g. For GO, seven pump wavelengths have been chosen: 330 nm, 400 nm, 460 nm, 510 nm, 560 nm, 600 nm, and 650 nm. From these experiments, a broad excited-state absorption signal from around 470 nm to 850 nm was observed, as well as two unexpected bleaching signals. One of the ground bleaching signals around 420 nm is independent of excitation. The other, which variably occurs in the visible light range at 480 nm, 500 nm, 540 nm, 580 nm, and 640 nm, is pump-wavelength dependent. It is worth noting that even though the energy of pump light is not large enough to directly excite the state in the blue side, this high-energy state always occurred and was accompanied with the excitation-wavelength-dependent low-energy states. Since the expected size effect of sp^2 clusters, we attribute the pump wavelength-dependent states to quantum-confined graphene-like states of differing sizes.

Three unique features of the signals of confined graphene-like states in GO are revealed. First, despite the disturbance of

excited-state absorption signal, the location of bleaching peaks in the 510–650 nm excitations is almost the same as the excitation wavelength, which is similar to band-edge excitation in traditional semiconductor quantum dots.[40] This is in accordance with the proposed physical picture of selective excitation of GO. At the same time, the spectral shape of the bleaching signals that refer to confined graphene-like states does not change during decay. This indicates that no energy relaxation occurs, which corresponds to carrier tunneling between these excited sp^2 clusters. Otherwise, the spectral shape of excited confined graphene-like states should be red-shifted as decay time from the location of small sp^2 cluster to a large one. Second, the experiment in 460 nm excitation shows an exceptional spectral mode, since it appears a bleaching peak at 480 nm in the red side of pump wavelength. This suggests that the carriers generated by 400–480 nm light pump have the possibility of falling into lower-energy sp^2 clusters with a bandgap at 2.58 eV (480 nm) in GO. This bandgap is close to the recent analysis results from incident photon to current conversion efficiency and linear potential scans of GO.[43] Therefore, this kind of unusual bleaching signal mode directly indicates the bandgap of GO. This also means that ultrafast broadband transient absorption spectroscopy excited in visible light range can be used for detecting the bandgap of GO as well as rGO (see below). Last but not least, the carrier dynamics in all these sp^2 domains are almost the same (Figure 2h). This implies that all of these sp^2 clusters have nearly same environment, namely, the surrounding sp^3 matrix in the vicinity, in which the interaction between sp^2 domains and sp^3 matrix dominates these ultrafast carrier dynamics. These features clearly indicate that most photogenerated carriers in GO are trapped in discrete sp^2 domains owing to the strong interplay with sp^3 matrix, which makes GO almost insulated, but the details on the "sp^3 matrix" are still unclear.

To scrutinize the spectral species in the sp^3 matrix of GO, femtosecond selective excitation transient absorption experiments in oxidized GO (Figure S1, Supporting Information) and photothermally reduced GO (**Figure 3**a–e) are also performed. The first impact is, of course, the spectral shape of GO samples with different treatments, especially for the photothermally reduced GO. It exhibits the extremely weak excited-state
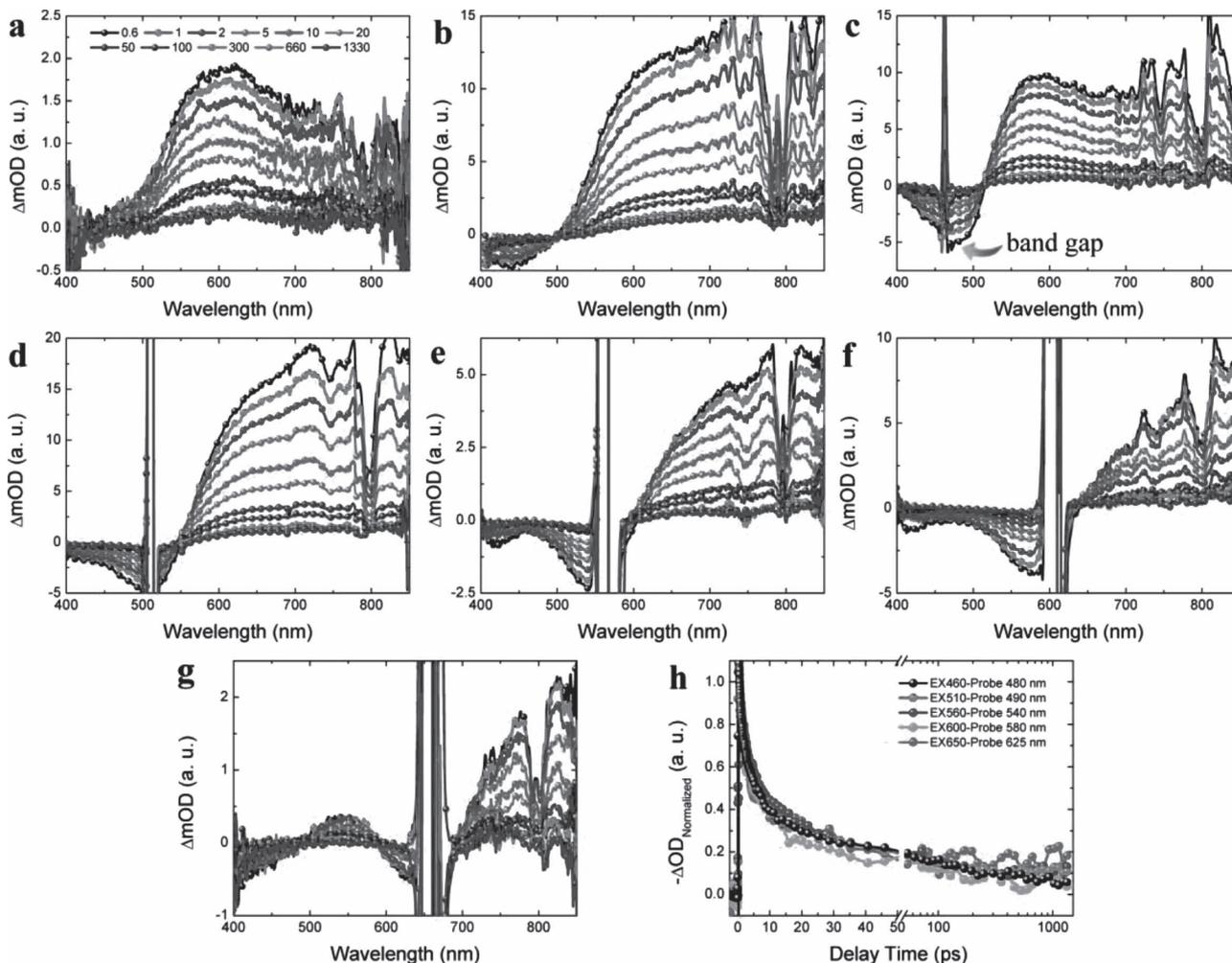
Figure 2. Transient spectral evolution of GO. Transient absorption spectra with picosecond unit in selective excitation wavelength: a) 330 nm, b) 400 nm, c) 460 nm, d) 510 nm, e) 560 nm, f) 600 nm, and g) 650 nm. The vertical lines in the visible light range are the scatters from the pump lights. The disturbances near 800 nm are from the limitation in probe light. h) Normalized carrier dynamics of sp^2 domains with different size.

absorption signal and the remarkable enhanced ratio of the bleaching signal of quantum-confined graphene-like states to bleaching signal in the blue side. Moreover, carrier dynamics in rGO are much faster than untreated and oxidized GO (Figure 3f), in which they are close to the reported carrier dynamics in pure graphene.[44–48]

A further detailed comparison and analysis help us to unambiguously identify these transient spectral characterizations. For the featureless excited-state absorption, a degree of oxidation–reduction-dependent spectral shape can be readily revealed: for example, the three samples (untreated GO, oxidized GO, and rGO) in the same condition of 330 nm excitation (**Figure 4**a). This indicates more reduction and smaller amplitude of entire excited-state absorption signals; contrarily, at around 600 nm, there is more oxidation and a larger excited-state absorption signal. Considering the large oscillator strength of oxygen-containing functional groups and calculated energy state for rich oxygen-containing functional groups area in GO, which are usually distributed in the high-energy region ($\geq$3.1 eV),[25,26] we

ascribe this broad excited-state absorption signal to the directly excited oxygen-containing functional groups. Interestingly, the different types of excited-state absorption before and after reduction could correspond to two kinds of oxygen-containing functional groups. One, which has a large excited-state absorption signal at around 600 nm, is easily removed; the other has a weak excited-state absorption signal in the near-infrared region and is thus hard to reduce. This evolution is also implied by the X-ray photoelectron spectroscopy (XPS) characterization of C1s for GO and rGO in Figure S2, Supporting Information. Since previous theoretical work indicates that epoxy groups are more stable than hydroxyl groups in GO under thermal reduction,[49] our results suggest the excited-state absorption signal at around 600 nm is mainly originated from hydroxyl groups, and the excited-state absorption signal in the near-infrared region could be attributed to epoxy groups and carbonyl groups.

However, when we excited GO using a low-energy light—that is, in 560 nm excitation (Figure 4b)—the state in the blue side occurred at the same time with confined states was
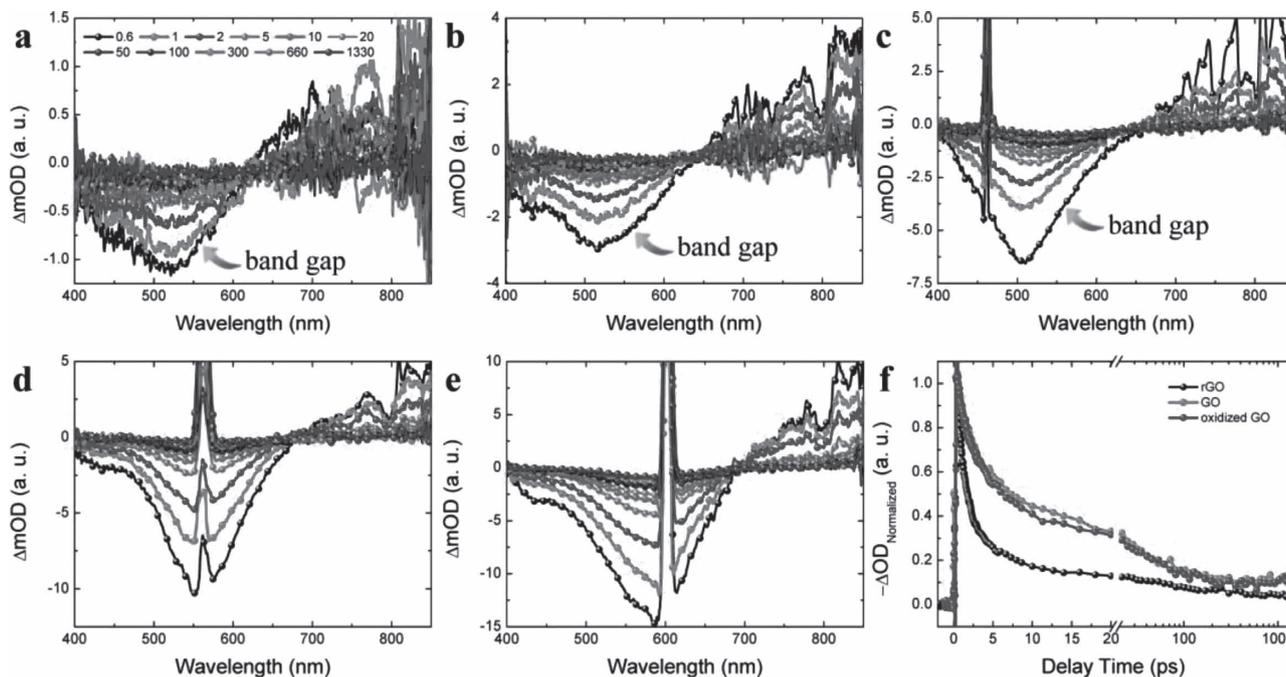
Figure 3. Transient spectral evolution of rGO. Transient absorption spectra with picosecond unit in selective excitation wavelength, a) 330 nm, b) 400 nm, c) 460 nm, d) 560 nm, and e) 600 nm. The vertical lines in the visible light range are the scatters from the pump lights. The disturbances near 800 nm are from the limitation in probe light. f) Normalized carrier dynamics probed at 540 nm of sp^2 domain in rGO in 560 nm excitation, in comparison with the carrier dynamics of sp^2 domain in GO and oxidized GO in same pump wavelength.

red-shifted with increasing degree of reduction from about 420 nm (2.95 eV) in untreated and oxidized GO to 435 nm (2.85 eV) in rGO. According to current first-principles calculations, the sole oxygen-containing functional group (hydroxyl, epoxy, or carbonyl) cannot be responsible for this state.[30,49] Fortunately, experimentally, this trend of dependence on the degree of oxidation–reduction is consistent with the reported bandgap in amorphous carbon with a high sp^3/sp^2 ratio.[50] This strongly implies that sp^3-hybridized carbon atoms bound to oxygen-containing functional groups can interact with quantum-confined graphene-like states to form a new hybrid state, which arises from disordered and ordered carbon atom arrangement. Our results suggest a new viewpoint to understand the role of functional groups. In this way, this still large enough hybrid state in rGO indicates that there are still many

disordered carbon atoms with sp^3 conformation in the vicinity of confined graphene-like states after removal of most oxygen-containing functional groups. This feature of lattice disorder is in agreement with Raman spectra analysis of GO and rGO (Figure S3, Supporting Information) and recent high-resolution transmission electron micrograph results.[21,22] In other words, the surrounding sp^3 matrix in the close vicinity of sp^2 clusters can not only provide a confinement potential but also spontaneously form an amorphous carbon-like peripheral structure with high sp^3/sp^2 carbon ratio.

Through the analyses discussed above, the transient spectral characterization of GO has been completely unraveled. In our opinion, GO is a kind of inhomogeneous single-atom-layer-thick, two-dimensional system. The isolated sp^2 domains, which are non-uniformly distributed in the entire GO sheet,
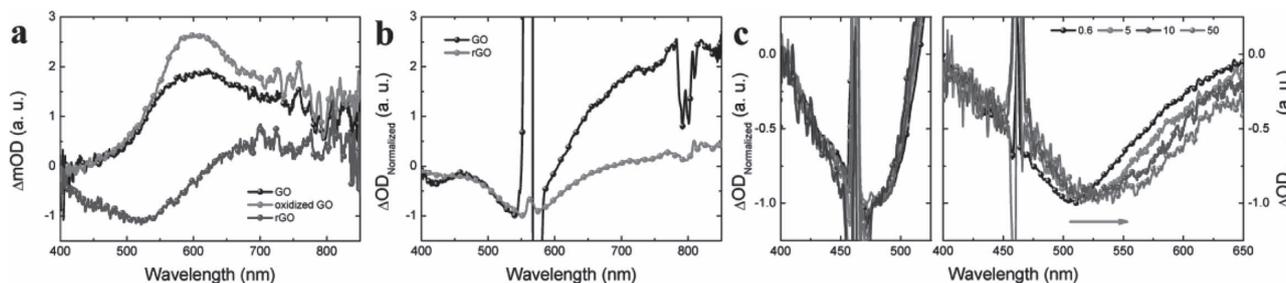

Figure 4. Detailed transient spectral comparison and analysis. A comparison in initial spectra for GO, oxidized GO and rGO in a) 330 nm and b) 560 nm excitation. c) Normalized bleaching signal evolution with picosecond unit for GO (left) and rGO (right) in 460 nm excitation. The vertical lines in the visible light range are the scatters from the pump lights. The disturbances near 800 nm are from the limitation in probe light.

are strongly affected by their surrounding amorphous carbon-like matrix with high sp^3/sp^2 ratio. Thus, the next question is how to understand the rGO. As it is electronically different from GO, rGO is usually considered to be a semi-metal with a finite density of states at the Fermi level.[1,51] Our experimental results also confirm this transition from "insulator" to semiconductor with gradual photothermal reduction. The transient spectra of modestly reduced GO are shown in Figure S4a,b, Supporting Information. In the 400 nm excitation, the width of bleaching signals referring to sp^2 domains as well as their carrier dynamics gradually increases with reduction (Figure S4c, Supporting Information). In Figure 4c, the normalized confined graphene-like states of rGO taken as an example in 460 nm excitation clearly indicate a fast spectral red-shift in contrast to GO in the same excitation condition. It reflects that the photogenerated carriers in small sp^2 clusters can quickly hop into the larger sp^2 clusters at 560 nm (2.21 eV) for this rGO sample. In higher-energy excitation, similar transient spectra with a red edge at around 560 nm occur again and again as the arrows indicated in Figure 3a–c. This means that as long as the excitation energy is larger than a special value, the photogenerated carriers in a high-energy level can relax into the same low-energy level. These behaviors provide direct spectral evidence unambiguously indicating that the photothermally reduced GO has semiconductor-like properties with a certain bandgap dependent on the degree of reduction. This physical picture also highlights that there are still many isolated large sp^2 domains in rGO, even if some parts of locations have been changed to be like semiconductor during the reduction processes.

Finally, according to these findings in GO and our previous study in green-fluorescence graphene quantum dots, in which we found an electronic state at about 410 nm,[35] we discuss some interesting photophysics in these oxygen-containing carbon nanomaterials (that is, graphene oxide, carbon dots, and graphene quantum dots). The transient absorption spectra of electrochemically fabricated carbon dots[52] are presented in **Figure 5**a,b. A similar phenomenon is that at 320 nm excitation, there is only a broad excited-state absorption signal, while at 400 nm excitation, a ground-state bleaching signal at around 420 nm occurs again, accompanied with the wide excited-state absorption signal. We collect the transient spectral feature of GQDs, GO, oxidized GO, and carbon dots together in Figure 5c.

Since we have assigned the state around 420 nm to the amorphous carbon-like peripheral structure with a high sp^3/sp^2 carbon ratio in the vicinity of sp^2 clusters and the excited-state absorption signal to oxygen-containing functional groups in GO, our results strongly suggests this conclusion can extend to GQDs and carbon dots. Owing to the different shape and peak location for the excited-state absorption signal, it implies different composition or distribution of oxygen-containing functional groups in various carbon nanomaterials. However, for the hybrid state, it implies that among these samples, the green-fluorescence GQDs have the highest disordered degree and least amount of functional groups owing to the smallest amplitude of this signal (at 410 nm, details in Wang et al.[35]), and the disordered degree of electrochemically fabricated carbon dots is similar to sheet-like GO and oxidized GO (at ≈420 nm). This suggests although the category or distribution of functional groups are different in oxygen-containing carbon nanomaterials, the similar hybrid interaction at the boundary of carbon nanoparticles creates a certain pattern in their transient spectra. This also implies further work could utilize these kinds of transient spectra as fingerprint to check other carbon nanomaterials if a database about the transient spectrum of graphene nanosheet with special oxygen-containing functional group has been finished. In addition, this common feature in these carbon nanomaterials revealed by transient absorption spectroscopy may be helpful for understanding the PL mechanism in carbon nanomaterials and Si quantum dots.[53–55]

In summary, through femtosecond selective excitation from ultraviolet to visible in broadband transient absorption spectroscopy, we unambiguously identify the transient spectral signals of discrete, quantum-confined graphene-like electronic states as well as the amorphous carbon-like peripheral structure with high sp^3/sp^2 carbon ratio in the vicinity of confined graphene-like states in GO. A "charge separation" mechanism could exist between these electronic states in close vicinity. This could be helpful for highly active photocatalytic processes.[43,56] It also renews the understanding of role of oxygen-containing functional groups in GO and its part-reduced derivatives. Moreover, a greater understanding of the fundamental physics of carbon nanomaterials will eventually be a benefit for design and fabrication of novel carbon-based nano optical-electronic devices in the not-too-distant future.
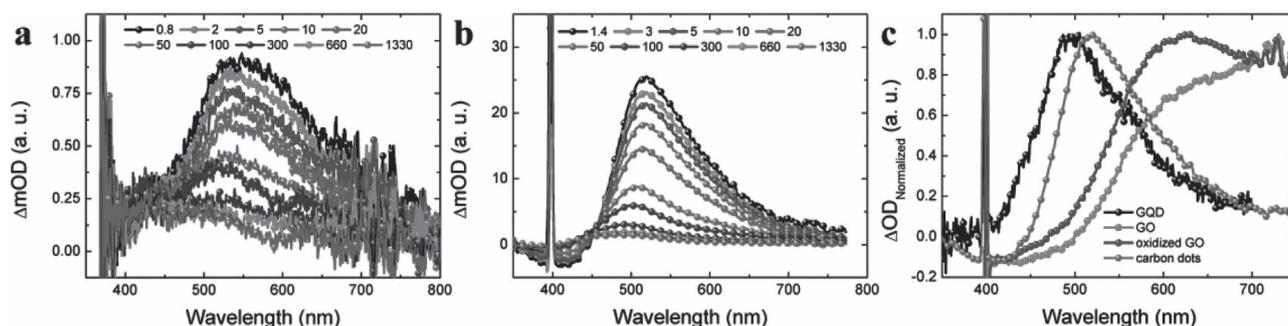

Figure 5. Transient spectral evolution of electrochemically fabricated carbon dots. Transient absorption spectra with picosecond unit for electrochemically fabricated carbon dots in a) 320 nm and b) 400 nm excitation, respectively. c) Initial transient spectra for green-fluorescence GQD, GO, oxidized GO, and electrochemically fabricated carbon dots in 400 nm excitation. Note that for the transient spectrum of GQD, the contribution of stimulated emission is subtracted. Details for GQD see our previous work.[35] The vertical lines in the visible light range are the scatters from the pump lights.

Experimental Section

Femtosecond Transient Absorption Setup: In the transient absorption setup, a mode-locked Ti:sapphire laser/amplifier system (Solstice, Spectra-Physics) was used. The output of the amplifier of 1.5 mJ pulse energy, 100 fs pulse width, 250 Hz repetition rate, at 800 nm wavelength is split into two parts; through the TOPAS system, the stronger beam was used to generate desired excitation light from ultraviolet to visible. In traditional 400 nm excitation experiments, 400 nm pump pulses directly doubled from 800 nm laser pulses. The broadband white-light probe pulses from 400 to 850 nm generated from 2-mm-thick water or 5-mm-thick CaF_2 substrate. The transient absorption data were collected by a fiber-coupled spectrometer connected to a computer. The group velocity dispersion of the transient spectra was compensated by a chirp program. In all experiments, clear sample solutions are used. All of the measurements were carried out at room temperature. Pump-power-dependent measurements were carried out: in the acceptable range (100–250 nJ pulse^{-1}), no pump-intensity-dependent dynamics were observed in 400 nm excitation.

Supporting Information

Supporting Information is available from the Wiley Online Library or from the author.

Acknowledgements

[1] K. P. Loh, Q. L. Bao, G. Eda, M. Chhowalla, *Nat. Chem.* **2010**, *2*, 1015.
[2] Y. L. Zhang, L. Guo, S. Wei, Y. Y. He, H. Xia, Q. D. Chen, H. B. Sun, F. S. Xiao, *Nano Today* **2010**, *5*, 15.
[3] D. Chen, H. B. Feng, J. H. Li, *Chem. Rev.* **2012**, *112*, 6027.
[4] G. Eda, M. Chhowalla, *Adv. Mater.* **2010**, *22*, 2392.
[5] Y. L. Zhang, Q. D. Chen, H. Xia, H. B. Sun, *Nano Today* **2010**, *5*, 435.
[6] Y. L. Zhang, Q. D. Chen, Z. Jin, E. Kim, H. B. Sun, *Nanoscale* **2012**, *4*, 4858.
[7] Q. M. Ji, I. Honma, S. M. Paek, M. Akada, J. P. Hill, A. Vinu, K. Ariga, *Angew. Chem. Int. Ed.* **2010**, *49*, 9737.
[8] Z. Q. Wei, D. B. Wang, S. Kim, S. Y. Kim, Y. K. Hu, M. K. Yakes, A. R. Laracuente, Z. T. Dai, S. R. Marder, C. Berger, W. P. King, W. A. de Heer, P. E. Sheehan, E. Riedo, *Science* **2010**, *328*, 1373.
[9] X. Wang, L. J. Zhi, K. Müllen, *Nano Lett.* **2008**, *8*, 323.
[10] C. Mattevi, G. Eda, S. Agnoli, S. Miller, K. A. Mkhoyan, O. Celik, D. Mastrogiovanni, G. Granozzi, E. Garfunkel, M. Chhowalla, *Adv. Funct. Mater.* **2009**, *19*, 2577.
[11] Q. Su, S. P. Pang, V. Alijani, C. Li, X. L. Feng, K. Müllen, *Adv. Mater.* **2009**, *21*, 3191.
[12] Y. F. Xu, Z. B. Liu, X. L. Zhang, Y. Wang, J. G. Tian, Y. Huang, Y. F. Ma, X. Y. Zhang, Y. S. Chen, *Adv. Mater.* **2009**, *21*, 1275.
[13] M. de Miguel, M. Álvaro, H. García, *Langmuir* **2012**, *28*, 2849.
[14] C. M. Hill, Y. Zhu, S. L. Pan, *ACS Nano* **2011**, *5*, 942.
[15] T. Kuilla, S. Bhadra, D. H. Yao, N. H. Kim, S. Bose, J. H. Lee, *Prog. Polym. Sci.* **2010**, *35*, 1350.
[16] Z. Zhang, H. H. Chen, C. Y. Xing, M. Y. Guo, F. G. Xu, X. D. Wang, H. J. Gruber, B. L. Zhang, J. L. Tang, *Nano Res.* **2011**, *4*, 599.
[17] I. V. Lightcap, P. V. Kamat, *J. Am. Chem. Soc.* **2012**, *134*, 7109.
[18] G. Katsukis, J. Malig, C. Schulz-Drost, S. Leubner, N. Jux, D. M. Guldi, *ACS Nano* **2012**, *6*, 1915.
[19] S. Gilje, S. Han, M. S. Wang, K. L. Wang, R. B. Kaner, *Nano Lett.* **2007**, *7*, 3394.
[20] C. Gómez-Navarro, R. T. Weitz, A. M. Bittner, M. Scolari, A. Mews, M. Burghard, K. Kern, *Nano Lett.* **2007**, *7*, 3499.
[21] C. Gómez-Navarro, J. C. Meyer, R. S. Sundaram, A. Chuvilin, S. Kurasch, M. Burghard, K. Kern, U. Kaiser, *Nano Lett.* **2010**, *10*, 1144.
[22] K. Erickson, R. Erni, Z. Lee, N. Alem, W. Gannett, A. Zettl, *Adv. Mater.* **2010**, *22*, 4467.
[23] G. Eda, Y. Y. Lin, C. Mattevi, H. Yamaguchi, H. A. Chen, I. S. Chen, C. W. Chen, M. Chhowalla, *Adv. Mater.* **2010**, *22*, 505.
[24] D. W. Boukhvalov, M. I. Katsnelson, *J.Am. Chem. Soc.* **2008**, *130*, 10697.
[25] J. A. Yan, L. D. Xian, M. Y. Chou, *Phys. Rev. Lett.* **2009**, *103*, 086802.
[26] R. J. W. E. Lahaye, H. K. Jeong, C. Y. Park, Y. H. Lee, *Phys. Rev. B* **2009**, *79*, 125435.
[27] W. Gao, L. B. Alemany, L. J. Ci, P. M. Ajayan, *Nature Chem.* **2009**, *1*, 403.
[28] A. Bagri, C. Mattevi, M. Acik, Y. J. Chabal, M. Chhowalla, V. B. Shenoy, *Nature Chem.* **2010**, *2*, 581.
[29] P. Johari, V. B. Shenoy, *ACS Nano* **2011**, *5*, 7640.
[30] P. V. Kumar, M. Bernardi, J. C. Grossman, *ACS Nano* **2013**, *7*, 1638.
[31] S. Wang, L. A. L. Tang, Q. L. Bao, M. Lin, S. Z. Deng, B. M. Goh, K. P. Loh, *J.Am. Chem. Soc.* **2009**, *131*, 16832.
[32] J. Lu, J. X. Yang, J. Z. Wang, A. L. Lim, S. Wang, K. P. Loh, *ACS Nano* **2009**, *3*, 2367.
[33] S. J. Zhu, J. H. Zhang, X. Liu, B. Li, X. F. Wang, S. J. Tang, Q. N. Meng, Y. F. Li, C. Shi, R. Hu, B. Yang, *RSC Adv.* **2012**, *2*, 2717.
[34] S. J. Zhu, S. J. Tang, J. H. Zhang, B. Yang, *Chem.Commun.* **2012**, *48*, 4527.
[35] L. Wang, S. J. Zhu, H. Y. Wang, Y. F. Wang, Y. W. Hao, J. H. Zhang, Q. D. Chen, Y. L. Zhang, W. Han, B. Yang, H. B. Sun, *Adv. Optical Mater.* **2013**, *1*, 264.
[36] S. Kaniyankandy, S. N. Achary, S. Rawalekar, H. N. Ghosh, *J. Phys. Chem. C* **2011**, *115*, 19110.
[37] Z. B. Liu, X. Zhao, X. L. Zhang, X. Q. Yan, Y. P. Wu, Y. S. Chen, J. G. Tian, *J. Phys. Chem. Lett.* **2011**, *2*, 1972.
[38] J. Z. Shang, L. Ma, J. W. Li, W. Ai, T. Yu, G. G. Gurzadyan, *Sci. Rep.* **2012**, *2*, 792.
[39] A. L. Exarhos, M. E. Turk, J. M. Kikkawa, *Nano Lett.* **2013**, *13*, 344.
[40] L. Wang, H. Y. Wang, B. R. Gao, L. Y. Pan, Y. Jiang, Q. D. Chen, W. Han, H. B. Sun, *IEEE J. Quantum Electron.* **2011**, *47*, 1177.
[41] L. Wang, H. Y. Wang, H. H. Fang, H. Wang, Z. Y. Yang, B. R. Gao, Q. D. Chen, W. Han, H. B. Sun, *Adv. Funct. Mater.* **2012**, *22*, 2783.
[42] Y. W. Hao, H. Y. Wang, Y. Jiang, Q. D. Chen, K. Ueno, W. Q. Wang, H. Misawa, H. B. Sun, *Angew. Chem. Int. Ed.* **2011**, *50*, 7824.
[43] T. F. Yeh, S. J. Chen, C. S. Yeh, H. S. Teng, *J. Phys. Chem. C* **2013**, *117*, 6516.
[44] L. B. Huang, G. V. Hartland, L. Q. Chu, Luxmi, R. M. Feenstra, C. X. Lian, K. Tahy, H. L. Xing, *Nano Lett.* **2010**, *10*, 1308.
[45] J. H. Strait, H. N. Wang, S. Shivaraman, V. Shields, M. Spencer, F. Rana, *Nano Lett.* **2011**, *11*, 4902.
[46] D. Sun, G. Aivazian, A. M. Jones, J. S. Ross, W. Yao, D. Cobden, X. D. Xu, *Nat. Nanotech.* **2012**, *7*, 114.
[47] S. Winnerl, M. Orlita, P. Plochocka, P. Kossacki, M. Potemski, T. Winzer, E. Malic, A. Knorr, M. Sprinkle, C. Berger, W. A. de Heer, H. Schneider, M. Helm, *Phys. Rev. Lett.* **2011**, *107*, 237401.
[48] L. Prechtel, L. Song, D. Schuh, P. Ajayan, W. Wgscheider, A. W. Holleitner, *Nat. Commun.* **2012**, *3*, 646.

[49] S. Y. Xie, X. B. Li, Y. Y. Sun, Y. L. Zhang, D. Han, W. Q. Tian, W. Q. Wang, Y. S. Zheng, S. B. Zhang, H. B. Sun, *Carbon* **2013**, *52*, 122.

[50] C. Mathioudakis, G. Kopidakis, P. C. Kelires, P. Patsalas, M. Gioti, S. Logothetidis, *Thin Solid Films.* **2005**, *482*, 151.

[51] G. Eda, C. Mattevi, H. Yamaguchi, H. Kim, M. Chhowalla, *J. Phys. Chem. C* **2009**, *113*, 15768.

[52] Y. L. Zhang, L. Wang, H. C. Zhang, Y. Liu, H. Y. Wang, Z. H. Kang, S. T. Lee, *RSC Adv.* **2013**, *3*, 3733.

[53] L. Cao, M. J. Meziani, S. Sahu, Y. P. Sun, *Account. Chem. Res.* **2013**, *46*, 171.

[54] K. Dohnalová, A. N. Poddubny, A. A. Prokofiev, W. DAM. de Boer, C. P. Umesh, J. MJ. Paulusse, H. Zuilhof, T. Gregorkiewicz, *Light: Sci. Appl.* **2013**, *2*, e47.

[55] W. D. A. M. de Boer, D. Timmerman, K. Dohnalová, I. N. Yassievich, H. Zhang, W. J. Buma, T. Gregorkiewicz, *Nat. Nanotech.* **2010**, *5*, 878.

[56] Y. J. Gao, G. Hu, J. Zhong, Z. J. Shi, Y. S. Zhu, D. S. Su, J. G. Wang, X. H. Bao, D. Ma, *Angew. Chem. Int. Ed.* **2013**, *52*, 2019.